Investigation of Tapered Roller Bearing Damage Detection Using Oil Debris Analysis

Paula J. Dempsey
NASA Glenn Research Center
Cleveland, OH 44135
paula.j.dempsey@nasa.gov

Gary Kreider and Thomas Fichter
The Timken Company
North Canton, OH 44720
gary.kreider@timken.com
tom.fichter@timken.com

Abstract—A diagnostic tool was developed for detecting fatigue damage to tapered roller bearings. Tapered roller bearings are used in helicopter transmissions and have potential for use in high bypass advanced gas turbine aircraft engines. This diagnostic tool was developed and evaluated experimentally by collecting oil debris data from failure progression tests performed by The Timken Company in their Tapered Roller Bearing Health Monitoring Test Rig. Failure progression tests were performed under simulated engine load conditions. Tests were performed on one healthy bearing and three predamaged bearings. During each test, data from an on-line, in-line, inductance type oil debris sensor was monitored and recorded for the occurrence of debris generated during failure of the bearing. The bearing was removed periodically for inspection throughout the failure progression tests. Results indicate the accumulated oil debris mass is a good predictor of damage on tapered roller bearings. The use of a fuzzy logic model to enable an easily interpreted diagnostic metric was proposed and demonstrated.

TABLE OF CONTENTS

1. INTRODUCTION

Oil analysis is one diagnostic tool used to indicate transmission and turbine engine health [1]. Bearing fatigue failures in helicopter transmissions and aircraft turbine engines generate significant debris in their lubrication systems. Oil debris monitoring for detecting damaged bearings in engines and transmissions consists of periodic off-line analysis of oil samples, magnetic chip detectors that capture the ferrous particles from the oil line and inductance type on-line oil debris sensors that monitor disturbance to a magnetic field as debris particles pass through the sensor.

Analysis of data from oil debris sensors often requires expert analysis of data. False alarms of oil debris technologies can be caused by non-failure debris. This debris can bridge the gap of plug type chip detectors. Inductance type oil debris sensors cannot differentiate between debris generated by a failing component and debris due to operational conditions [2].

Monitoring the debris in the lubrication systems with an inductance type oil debris sensor has been successfully used to indicate damage to critical components in aircraft engines [3]. Several companies manufacture inductance type oil debris sensors that measure debris size and count particles [4]. The oil debris sensor selected for this research was used in a previous analysis, and results demonstrated the debris mass measured by the sensor showed a significant increase when gear and bearing pitting damage began to occur [5-8]. Earlier work performed at Timken also showed the particles measured by the inductance oil debris monitoring system (ODM) could provide early indication of impending failures during tapered roller bearing failure progression rig testing [9,10]. Further failure progression testing is required to define warning levels using oil debris analysis.

The objective of the work reported herein is to first identify the best feature for detecting tapered roller bearing damage from a commercially available in-line, real-time, inductance type oil debris sensor. Once a feature for detecting bearing damage is defined through analysis of the oil debris data collected during failure progressions tests, a method for setting threshold limits for varying magnitudes of damage to the bearings will be identified.

2. TEST FACILITY DESCRIPTION

Failure progression tests were conducted in the Tapered Roller Bearing Health Monitoring Test Rig at Timken. The test rig is illustrated in Figure 1.

[2] IEEEAC paper #1119, Version 2, Updated Dec, 16 2005

The test rig consists of two tapered bearings supported on the shaft. The test bearing was at the load cylinder end and the slave bearing at the motor end. The test and support bearings are loaded in the axial direction with a hydraulic load cylinder. A 200 hp electric motor is used to drive the test system to the required rpm. There is a direct drive connection from the motor to the bearing shaft, with a small coupling shaft connecting the two that compensates for minor misalignment. Mobil Jet II oil (per MIL-L-23699 specifications) was used as the lubricant. Bearing geometry information is listed in Table 1.

During failure progression tests, each bearing is loaded to an axial load of 40,000 lbf. The cylinder is applying the 40,000 lbf which is seen by each bearing. The axial dynamic load thrust rating for each bearing is 28,559 lbf. The shaft speed is 3200 rpm. Tests are performed until a significant amount of debris is measured by the ODM. The test rig is instrumented to measure cup temperatures, input oil temperatures, oil flow rates, speed and torque. Vibration data was also collected from accelerometers located on the test bearing housing in the radial, axial horizontal and vertical positions.

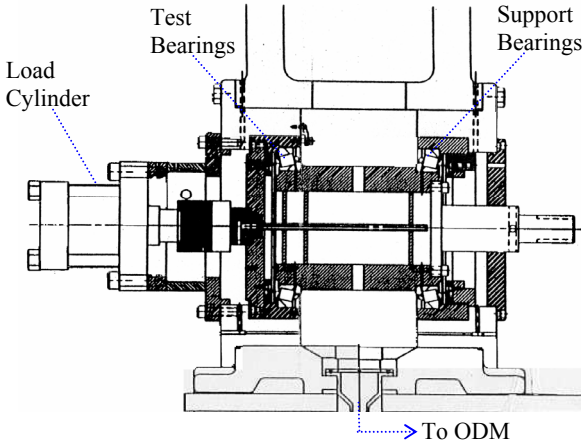

Figure 1 - Tapered roller bearing test rig.

Table 1. Bearing Dimensions

No. of Rolling Elements	Mean Roller Diameter (in.)	Brg. Pitch Diameter (in.)	Contact Angle (deg)
29	1.21	14.72	13.07

Oil debris data were collected from a 1-1/4 in. ODM (Oil Debris Monitor) installed downstream of the bearing housing. A 120 µm screen mesh was installed downstream of the ODM. A 10 µm filter was also installed on the input oil line before the oil entered the bearings. The ODM measures the change in a magnetic field caused by passage of a metal particle where the amplitude of the sensor output signal is proportional to the particle mass. The sensor counts the number of particles, their approximate size based on user defined particle size ranges, and calculates an accumulated mass [11]. For these experiments, 16 size ranges, referred to as bins, were defined. Based on the bin configuration, the average particle size for each bin is used to calculate the cumulative mass for the experiment. The particle is assumed to be a sphere with a diameter equal to the average particle size. Table 2 lists the 16 particle size ranges and the average particle size used to calculate accumulated mass during bearing tests. Previous research verified accumulated mass is a good predictor of pitting damage and identified threshold limits that discriminate between stages of pitting on spur gears [6]. This method will be applied to the data collected during the failure progression tests.

Table 2. Ferrous oil debris particle size ranges

Bin	Bin range, µm	Average	Bin	Bin range, µm	Average
1	250–275	263	9	625–675	650
2	275–325	300	10	675–725	700
3	325–375	350	11	725–775	750
4	375–425	400	12	775–825	800
5	425–475	450	13	825–875	850
6	475–525	500	14	875-925	900
7	525–575	550	15	925-975	950
8	575–625	600	16	975-1016	995

An alternative technique recommended by the ODM manufacturer for setting oil debris mass alarm limits based on bearing damage will also be applied to the failure progression data [12]. This technique uses the bearing geometry to set an alarm threshold based on the total accumulated mass of the debris, M_{alarm}, as calculated in equation (1) below. This mass alarm limit is based on outer race damage, in which the outer race spall angle is large enough to allow 2 balls in the damaged portion at the same time. The calculation for this technique is shown below:

$$M_{alarm} = K \frac{360}{N_b} P_d B_d \qquad (1)$$

Where:
N_b = number of rolling elements = 29
P_d = bearing pitch diameter (in.) = 14.72
B_d = rolling element mean diameter (in.) = 1.21
K = constant for roller bearings (mg/deg in^2) = 9.31

The K factor was obtained experimentally by the sensor manufacturer based on data collected from over 40 bearing failures [12]. A K factor of 9.31 for roller bearings was used for this application. A mass alarm value of 2058 mg was calculated for the roller bearing. The manufacturer also provides a method to calculate mass warning, 0.1 times the mass alarm, 205.8 mg, to indicate initial spall development.

3. Results And Discussion

The analysis discussed in this section is based on data collected during testing of four tapered roller bearings, one

healthy bearing and three predamaged bearings. The principal focus of this research is the detection of damage progression on tapered roller bearings. The types of damage observed on the bearings included spalling, peeling and damage from foreign material. The photos of the amount of damage observed during each failure progression test and the analysis of the oil debris will be discussed in the following sections.

Bearing Test 1—After the bearing races were damaged by running in a contaminated oil containing steel powder particles for 2000 revolutions, they were then ultrasonically cleaned and installed in the test rig. The bearings were removed for inspection two times during the failure progression test. At test completion the bearings had been subjected to 81 million cycles. Figure 2 is a plot of the accumulated mass measured by the ODM during test 1. The boxes labeled 1 and 2 identify when the bearings were removed for inspection. Table 3 is a summary of the particle counts and accumulated mass measured in each bin prior to each inspection interval and at test completion.

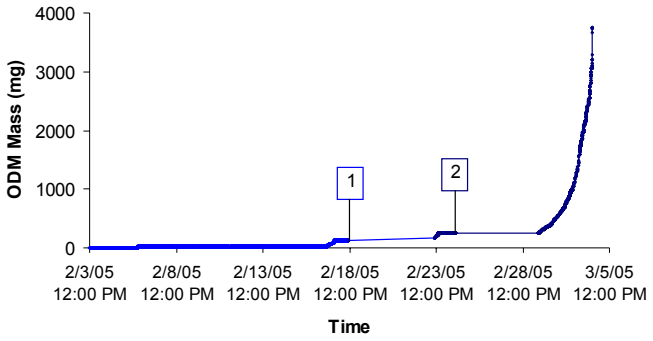

Figure 2 - Mass measured by the ODM during test 1.

Table 3. Test 1 Particle Distribution and Accumulated Mass

Bin	Bin range, µm	Inspect 1	Inspect 2	Test Complete
1	250–275	22	62	592
2	275–325	94	210	2424
3	325–375	54	143	1858
4	375–425	57	116	1215
5	425–475	16	44	741
6	475–525	17	48	468
7	525–575	8	24	333
8	575–625	14	20	256
9	625–675	4	9	168
10	675–725	9	12	146
11	725–775	1	2	75
12	775–825	0	2	72
13	825–875	2	3	47
14	875-925	0	3	47
15	925-975	0	0	0
16	975-1016	6	9	221
Mass (mg)		117.1	245.6	3752.6

Photos of the damaged components were taken at each inspection interval and at test completion. Photos of the damage are shown in Figures 3 through 6. After the first inspection interval, spalling was observed on several of the rollers and peeling was observed on the cup and cone. The spalls on the rollers increased in size during the second inspection, but the peeling on the cup and cone did not appear to increase significantly. At test completion, the spalls on the rollers increased significantly, the peeling on the cup and cone did not change, spalling began to occur on the cone and cage damage was also observed. It should be noted that the cage material of all bearings tested was silver, and nonferrous particles were not analyzed during these tests.

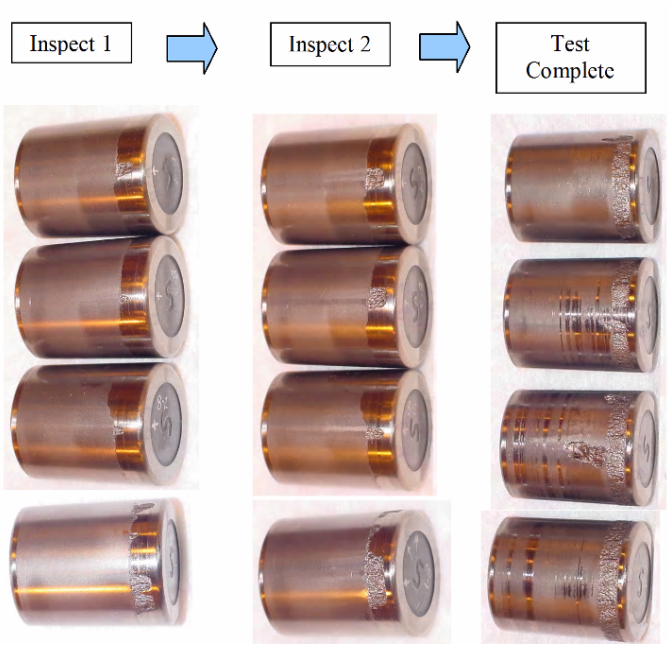

Figure 3 - Test 1 roller damage.

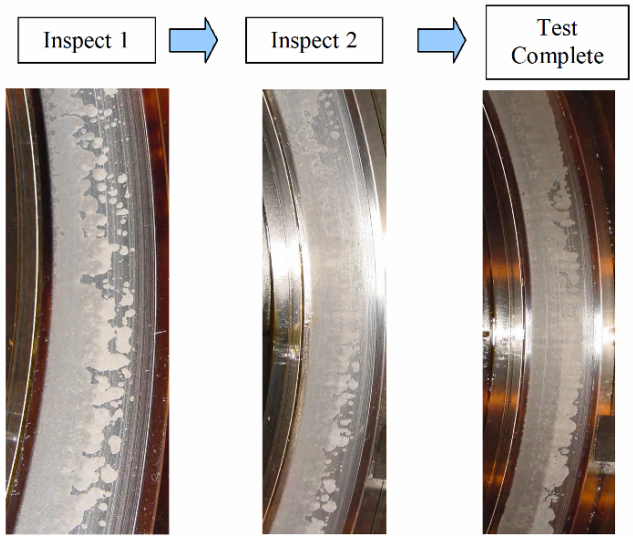

Figure 4 - Test 1 cup damage.

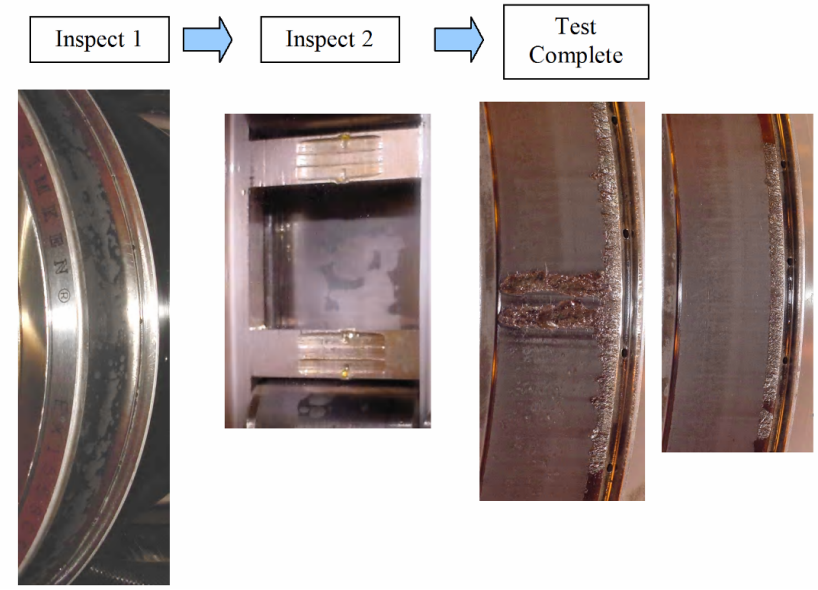

Figure 5 - Test 1 cone damage.

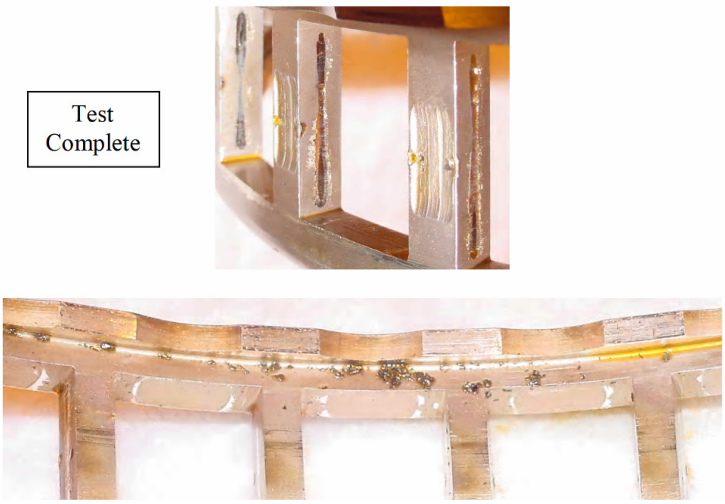

Figure 6 - Test 1 cage damage.

Bearing Test 2—After the bearing was predamaged by applying hardness dents to the cone, the bearings were loaded and installed in the test rig. The bearings were removed for inspection four times during the failure progression test. At test completion the bearings had been subjected to 92 million cycles. Figure 7 is a plot of the accumulated mass measured by the ODM during test 2. The boxes labeled 1 through 4 identify when the bearings were removed for inspection. Table 4 is a summary of the particle counts and accumulated mass measured in each bin prior to each inspection interval and at test completion.

Photos of the damaged components were taken at each inspection interval and at test completion. Photos of the damage are shown in Figures 8 to 12. After the first inspection interval, wear lines were observed on the rollers, and the dents slightly increased in size. During inspection 2, small pits were observed on the cup, no significant damage was observed on the rollers. At inspection interval 3, a large spall was observed on the cone and a few more wear lines on the rollers. At inspection interval 4, the cone spall increased in size. At test completion the cone spall doubled in size, the small pits observed on the cup at inspection 2 remained the same, and cage damage was observed.

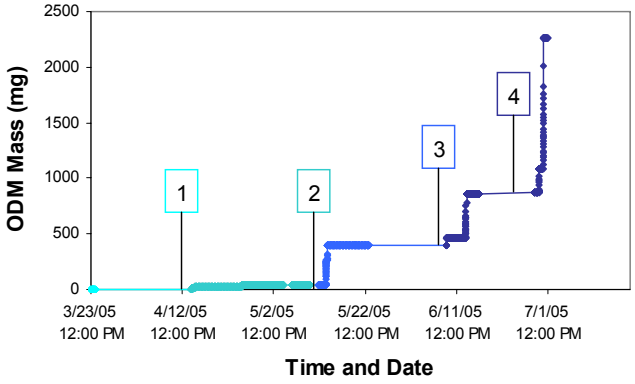

Figure 7 - Mass measured by the ODM during test 2.

Table 4. Test 2 Particle Distribution and Accumulated Mass

Bin	Bin range, µm	Inspect 1	Inspect 2	Inspect 3	Inspect 4	Test Complete
1	250–275	0	4	45	116	350
2	275–325	4	26	235	532	1765
3	325–375	2	10	156	342	1298
4	375–425	0	8	115	239	762
5	425–475	2	8	74	152	456
6	475–525	1	3	57	116	317
7	525–575	2	7	36	78	215
8	575–625	1	1	26	55	147
9	625–675	1	4	22	39	106
10	675–725	0	2	12	29	74
11	725–775	0	3	12	25	54
12	775–825	0	1	9	17	36
13	825–875	0	0	5	17	31
14	875-925	0	1	4	12	33
15	925-975	0	0	0	0	0
16	975-1016	0	1	24	52	109
Mass (mg)		5.4	38.7	394.0	860.4	2265.4

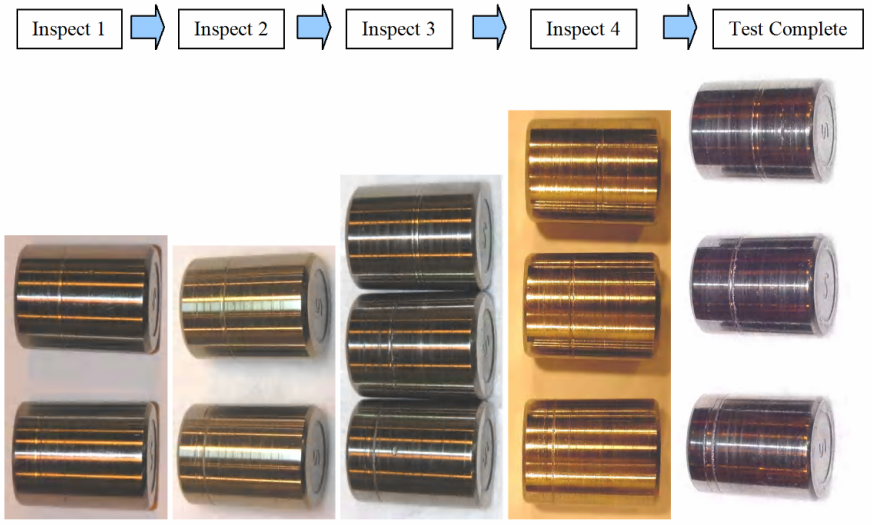

Figure 8 - Test 2 roller damage.

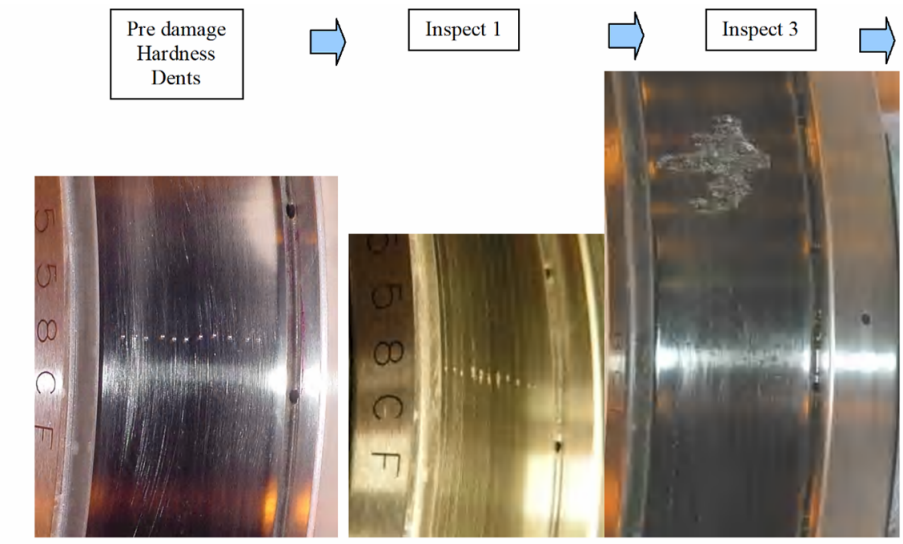

Figure 9 - Test 2 cone damage.

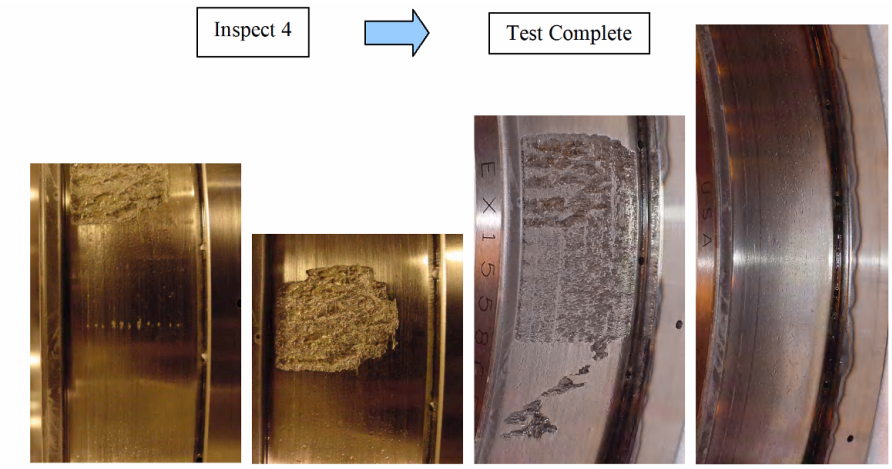

Figure 10- Test 2 cone damage.

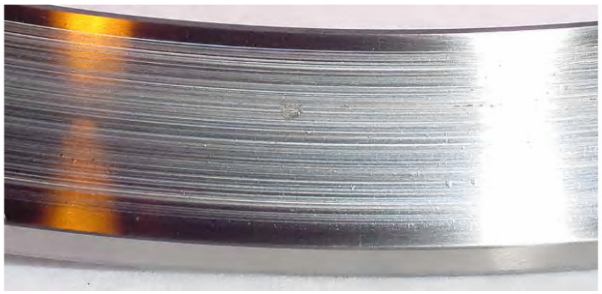

Figure 11 - Cup damage at test completion, observed after inspection 2, but did not progress.

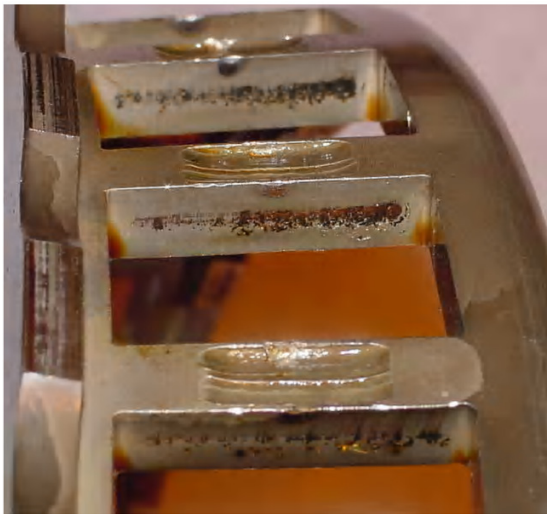

Figure 12 - Test 2 cage damage at test completion.

Bearing Test 3—After the bearing was predamaged by applying hardness dents to the cone, the bearings were loaded and installed in the test rig. The bearings were removed for inspection three times during the failure progression test. At test completion the bearings had been subjected to 168 million cycles. Figure 13 is a plot of the accumulated mass measured by the ODM during test 3. The boxes labeled 1 through 3 identify when the bearings were removed for inspection. Table 5 is a summary of the particle counts and accumulated mass measured in each bin prior to each inspection interval and at test completion.

Photos of the damaged components were taken at each inspection interval. Photos of the damage are shown in Figure 14. After the first inspection interval, no damage was observed on the bearing. In order to expedite failure, the raceway was again damaged near the original predamage hardness dents. During inspection 2, pitting damage began to occur near the location of the predamage dents and damage placed on the cone during inspection 1. At inspection interval 3, the damage observed on the cone during inspection 2 grew into a large spall. At test completion, the initial spall grew slightly and another spall occurred 90 degrees from the original spall and wear lines were observed on the rollers.

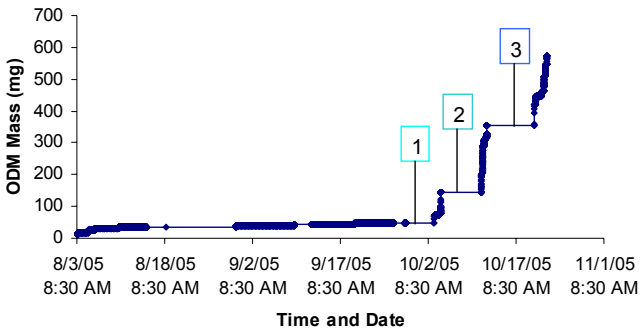

Figure 13 - Mass measured by the ODM during test 3

Table 5. Test 3 Particle Distribution and Accumulated Mass

Bin	Bin range, µm	Inspect 1	Inspect 2	Inspect 3	Test Complete
1	250–275	12	21	44	70
2	275–325	46	85	184	305
3	325–375	29	62	146	234
4	375–425	22	39	94	147
5	425–475	6	13	42	86
6	475–525	8	14	43	72
7	525–575	8	16	31	44
8	575–625	4	9	23	38
9	625–675	0	4	18	29
10	675–725	1	6	22	31
11	725–775	0	2	12	20
12	775–825	1	2	4	8
13	825–875	3	4	6	8
14	875-925	1	2	4	7
15	925-975	0	0	0	0
16	975-1016	0	11	23	38
Mass (mg)		46.0	142.9	353.5	573.5

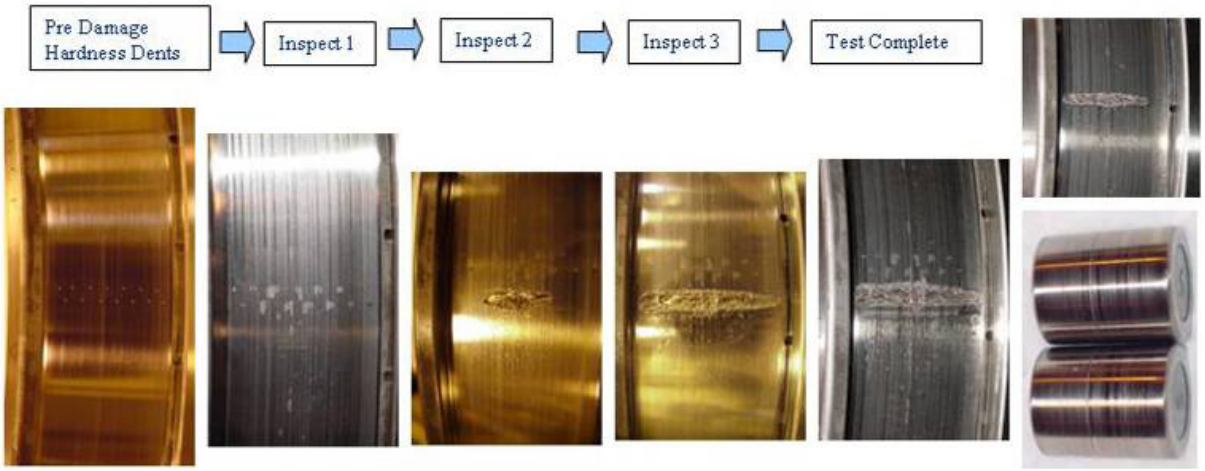

Figure 14 - Test 3 cone damage.

Baseline Test —A healthy set of bearings was also tested to determine baseline wear debris. The healthy set of bearings was installed at the completion of test 2. The load was gradually increase during testing. Figure 15 is a plot of the accumulated mass measured by the ODM during the baseline test. Table 6 is a summary of the particle counts and accumulated mass measured at test completion. The amount of debris detected was significant during this break in period.

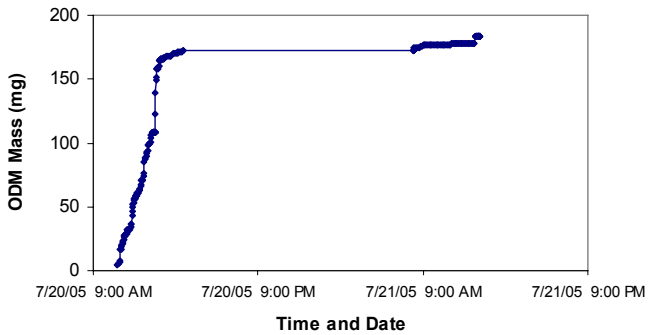

Figure 15 - Mass measured during baseline test

Table 6. Baseline Test Particle Distribution and Mass

Bin	Bin range, µm	Test Complete
1	250–275	18
2	275–325	92
3	325–375	113
4	375–425	63
5	425–475	46
6	475–525	28
7	525–575	17
8	575–625	14
9	625–675	11
10	675–725	8
11	725–775	7
12	775–825	7
13	825–875	2
14	875-925	3
15	925-975	0
16	975-1016	4
Mass (mg)		183.5

Due to the fact that different bearing components experienced different levels of damage during each test, particle size distributions were plotted to determine if particles distributions vary when different components in the bearing are damaged. Figures 16 through 19 are histograms of the three bearing tests and the baseline tests. The histograms show the frequency particles were measured within each size distribution. The histograms indicate inspection intervals and test completion particle distributions. It should be noted that when performing a particle distribution analysis on the oil debris data, the bin size ranges are critical to the results. A brief review of the figures show particle distributions are very similar at test completion and during the inspection intervals when spalling occurred on the cage and the rollers. During the inspection intervals when spalling damage was observed, the maximum particles were observed in the 275-325 µ bin range. During the baseline test, when no damage occurred, the maximum particles were observed in the 325-375 µ particle size range.

Size distribution characteristics were calculated from the histograms to attempt to capture the difference in distributions between the baseline test and the failure progression tests. Relative skewness and kurtosis of the particle distributions were calculated to determine if these statistical parameters could be used to differentiate between the damaged and undamaged bearing. Skewness is a

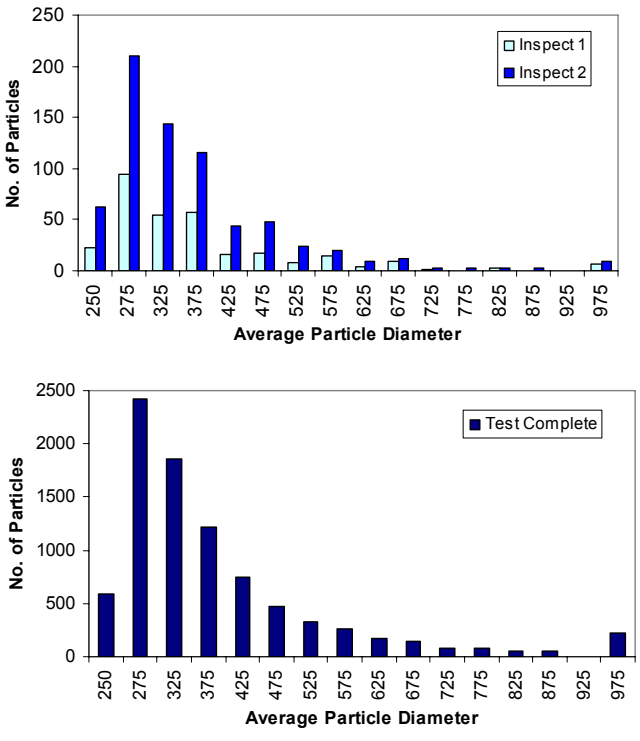

Figure 16 - Test 1 particle distributions after inspections 1 and 2 and at test completion.

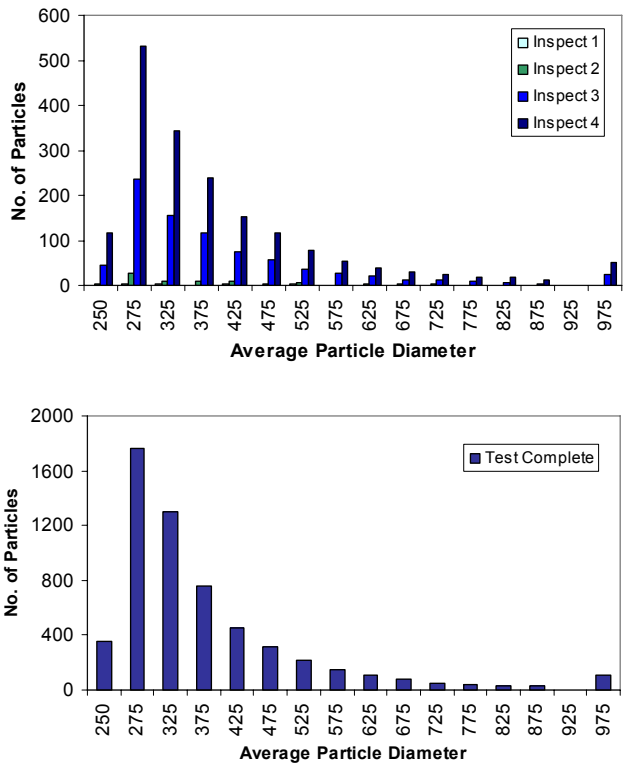

Figure 17 - Test 2 particle distributions after inspections 1-4 and at test completion.

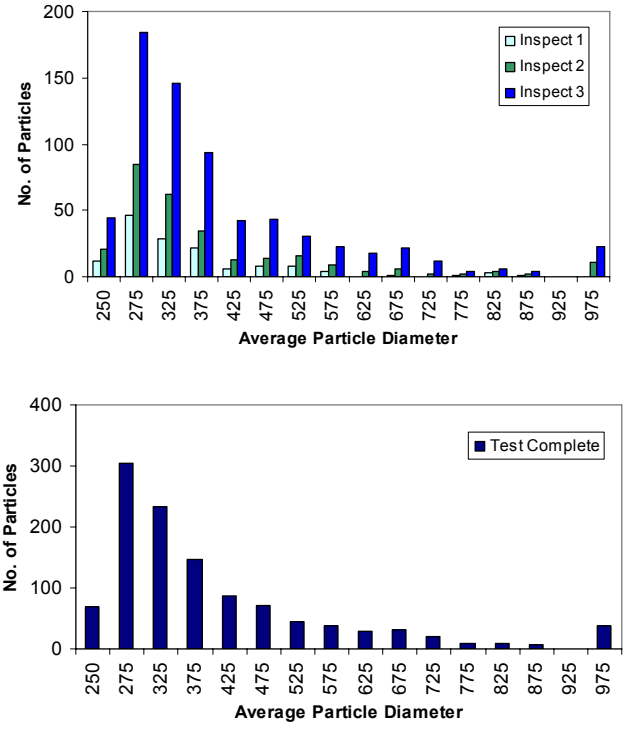

Figure 18 - Test 3 Particle distributions after inspections and at test completion.

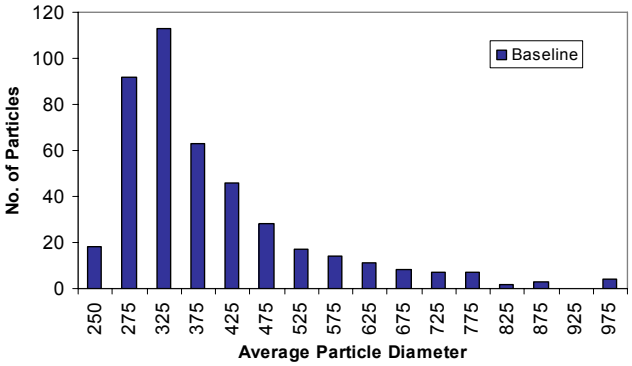

Figure 19 - Baseline particle distributions at test completion.

measure of the asymmetry of the histogram. All of the particle distributions show positive skewness, the tail on the right side of the distribution is longer. Kurtosis is a measure of the combined weight of the tails related to the rest of the distribution. As the tails become heavier, kurtosis increases.

The following equations were used to calculate relative kurtosis and relative skewness from the particle distributions shown in Figures 16 through 19 [13], where d_j is equal to average bin size, j is equal to the number of bins and $P[d_j]$ is equal to the particles per average bin size divided by total number of particles:

$$Mean\ particle\ size = E(d) = \sum_{j=1}^{N} d_j P\left[d_j\right] \tag{2}$$

$$Variance = \sum_{j=1}^{N} \left(d_j - E(d)\right)^2 P\left[d_j\right] \tag{3}$$

$$Kurtosis = \sum_{j=1}^{N} \left(d_j - E(d)\right)^4 P\left[d_j\right] \tag{4}$$

$$Skewness = \sum_{j=1}^{N} \left(d_j - E(d)\right)^3 P\left[d_j\right] \tag{5}$$

$$Relative\ Kurtosis = RK = \frac{Kurtosis}{(Variance)^2} \tag{6}$$

$$Relative\ Skewness = RS = \frac{Skewness}{(Variance)^{3/2}} \tag{7}$$

Results of the calculated relative kurtosis (RK) and relative skewness (RS) are listed in Table 7. Both calculated values were lower during test 2 inspection intervals 1 and 2 than they were for the baseline test. However, minimal wear damage was observed on the rollers during these two inspection intervals. Relative kurtosis was also lower for test 3 inspection interval 3 and test completion. Further analysis is required to determine if an increase in relative kurtosis of the particle distributions could be used as an oil debris feature for damage indication of the bearing.

In order to develop an oil debris feature that best predicts damage levels to the tapered roller bearings, the bearing damage levels or state of the bearing must be defined. Three primary states of the bearing health will focus on spalling damage: O.K. (no damage); Inspect (initial spalling); Damage (severe spalling). Next, initial limits for these damage levels must be defined. The oil debris mass data from the 3 experiments with damage were plotted on Figure 20. The red diamonds identify the inspection intervals during tests. Next, the plot is expanded, with the gear state transition regions expanded: O.K. (green); Inspect (yellow); Damage (red). Since spalling damage was not observed during test 2, inspection intervals 1 and 2, this mass (38.7 mg) will be used as the lower limit on the inspect region. The upper inspect band will be at 183.5 mg, the maximum mass measured at the baseline test completion. One interesting observation when reviewing Figure 20 is that the mass alarm value (M_{alarm}) of 2058 mg and the mass warning value 205.8 mg, calculated using the manufacturers equation (1), both fall within the damage region.

Fuzzy logic was used to develop a feature that defines damage levels based on the accumulated mass measured by the ODM. Fuzzy logic applies fuzzy set theory to data, where fuzzy set theory is a theory of classes with unsharp boundaries and the data belongs in a set based on its degree of membership [14]. The degree of membership can be any value between 0 and 1. Membership values based on the accumulated mass measured by the oil debris sensor will be identified.

Table 7. Relative Skewness and Kurtosis of Particle Distributions

	Baseline	Test 1 Insp. 1	Test 1 Insp. 2	Test 1 Complete	Test 2 Insp. 1	Test 2 Insp. 2	Test 2 Insp. 3	Test 2 Insp. 4	Test 2 Compl.	Test 3 Insp. 1	Test 3 Insp. 2	Test 3 Insp. 3	Test 3 Compl.
RS	1.70	2.06	2.15	2.01	0.30	1.31	1.82	1.84	2.12	2.00	1.87	1.70	1.74
RK	5.95	7.93	8.81	7.22	1.65	4.19	6.29	6.24	7.95	7.38	6.02	5.55	5.71

The data measured from the oil debris sensor during experiments with damage and with no damage was used to identify membership functions to build a simple fuzzy logic model. Defining the fuzzy logic model requires inputs (damage detection features), outputs (state of bearings), and rules. Inputs are the levels of damage, and outputs are the states of the bearings as discussed in the preceding paragraph. Membership values were based on the accumulated mass and the amount of damage observed during inspection. Membership values are defined for the three levels of damage: damage low, damage medium, and damage high. Using the Mean of the Maximum (MOM) fuzzy logic defuzzification method, the oil debris mass measured was input into a simple fuzzy logic model created using commercially available software [15]. The membership function and the output of this model are shown on Figure 21. Threshold limits for the accumulated mass are identified. Results from the four experiments indicate accumulated mass is a good predictor of pitting damage on tapered roller bearings and fuzzy logic is a good technique for setting threshold limits that discriminates between states of pitting wear.

4. CONCLUSIONS

The purpose of this research was to first verify, when using an inductance type, on-line, oil debris sensor, that accumulated mass correlates with tapered roller bearing fatigue damage. Then, using accumulated mass as the damage feature, a method was proposed and used to set threshold limits for damaged bearings that discriminates between different levels of pitting damage. In this process, the membership functions for each feature state were defined based on level of damage. From this data, accumulated mass measured by an oil debris sensor combined with fuzzy logic analysis techniques can be used to predict tapered roller health. Applying fuzzy logic incorporates decision-making into the diagnostic process that improves fault detection and decreases false alarms [7]. This approach has several benefits over using the accumulated mass and an arbitrary threshold limit for determining if damage has occurred. One is that it eliminates the need for an expert diagnostician to analyze and interpret the data, since the output would be one of three states, O.K., Inspect, and Shutdown. Since benign debris may be introduced into the system, due to periodic inspections, setting the lower limit to above this debris level will minimize false alarms. In addition to this, a more advanced system can be designed with logic built-in to minimize these operational effects. Future tests are required to collect data from bearings with initial pitting to better define the inspect region and the severity of bearing damage. Tests of bearings of different sizes are required to determine if a relationship can be developed between damage levels and bearing dimensions to minimize the need for extensive tests to develop the membership functions for the threshold levels.

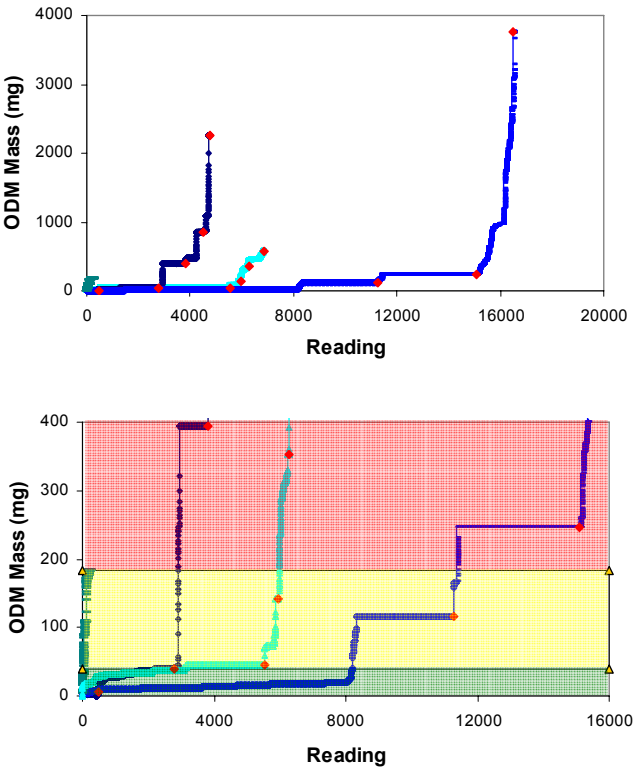

Figure 20 - Oil Debris mass during each experiment.

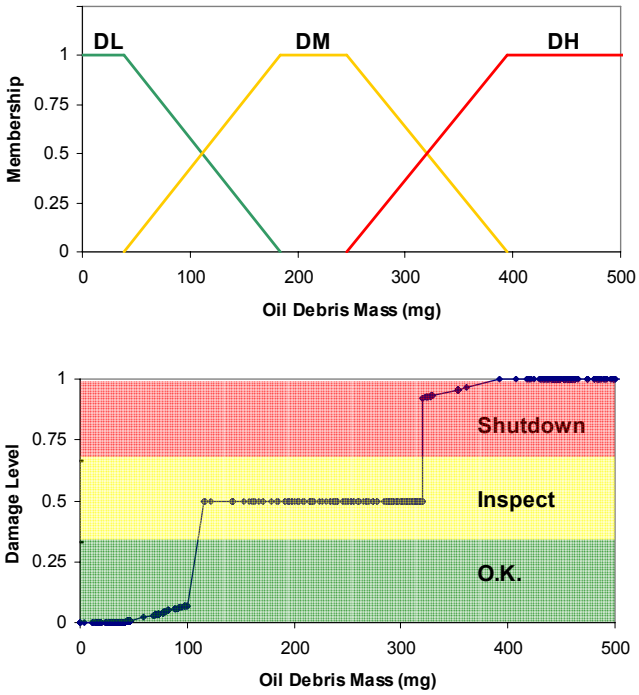

Figure 21 - Fuzzy logic membership values for oil debris feature and output of model.

REFERENCES

[1] Miller, J.L. and Kitaljevich, D.: In-line Oil Debris Monitor for Aircraft Engine Condition Assessment. IEEE 0–7803 5846–5/00.

[2] Howard, P.L., and Reintjes, J.: A Straw Man for the Integration of Vibration and Oil Debris Technologies. Presented at the Workshop on Helicopter Health and Usage Monitoring Systems, Melbourne, Australia, February 1999. Editor: Graham F. Forsyth. DSTO-GD-0197 published by DSTO (Defense Science and Technology Organization) Australia, February 1999.

[3] Dubowski, D. and Witwer, D.: Application of MetalSCAN Oil Debris Monitor to a Fleet of Sea King Helicopters. Presented at the American Helicopter Society 60th Annual Forum, Baltimore, MD, June 7–10, 2004.

[4] Hunt, T. M.: Handbook of Wear Debris Analysis and Particle Detection in Liquids. Elsevier Applied Science, London, 1993.

[5] Dempsey, P. J.: A Comparison of Vibration and Oil Debris Gear Damage Detection Methods Applied to Pitting Damage. NASA/TM—2000-210371.

[6] Dempsey, P.J.: Gear Damage Detection Using Oil Debris Analysis," NASA/TM—2001-210936, Sept. 2001. Published in the Journal of Gear Technology, January 2003.

[7] Dempsey, P.J.: Integrating Oil Debris and Vibration Measurements for Intelligent Machine Health Monitoring. PhD Thesis, The University of Toledo. Published in the Journal of the American Helicopter Society, April 2004, vol. 49, no. 2.

[8] Dempsey, P.J., Lewicki, D.G., and Decker, H.J.: Investigation of Gear and Bearing Fatigue Damage Using Debris Particle Distributions, NASA/TM—2004-212883, May 2004.

[9] Kreider, G.E.: Tapered Roller Bearing Health Monitoring Test for Pratt & Whitney. Application Development Summary Report Project No. 009921, January 2000.

[10] Kreider, G.E.: Tapered Roller Bearing Health Monitoring Test II for Pratt & Whitney. Application Development Summary Report Project No. 009921 Supplement 1, December 2000.

[11] Howe, B.; and Muir, D.: In-Line Oil Debris Monitor (ODM) for Helicopter Gearbox Condition Assessment. AD–a347 503, BFGoodrich.

[12] MetalSCAN™ User's Manual. Setting Alarm Limits, C000833, Revision 0, GasTOPS, Ontario, Canada.

[13] Roylance, B.J.: Monitoring Gear Wear Using Debris Analysis—Prospects for Establishing a Prognostic Method. Proceedings of the 5th International Congress on Tribology, vol. 4, June 15, 1989.

[14] Zadeh, Lofti, Fuzzy Logic: Advanced Concepts and Structures, New Jersey: IEEE, 1992.

[15] "Fuzzy Logic Toolbox for use with MATLAB," January 1998.

BIOGRAPHY

Paula Dempsey is an Aerospace Research Engineer employed by the NASA Glenn Research Center, Cleveland, Ohio. She joined NASA in 1991, after performing experimental and analytical research work in the area of cryogenic fluid management systems for a government contractor from 1987-1991. She continued her cryogenic research until 1995, then moved to Aeronautics research, serving as lead project engineer for several Aeronautics programs. Since 1998, she has been performing research in the area of health monitoring and diagnostics for aerospace drive systems and propulsion systems and has published over 20 papers in this field. She received her BS in Mechanical Engineering, an MS degree in Industrial Engineering and a Ph.D. in Engineering Science.

Gary Kreider is a Senior Product Development Specialist employed by The Timken Company, Canton, Ohio. He joined The Timken Company in 1967 as an application engineer working on bearing applications for automotive and rotary wing aircraft. In 1982 he joined the Timken Company's Physical Laboratory serving as a project leader for bearing development in industrial, agriculture and aerospace programs. The latter involving hybrid tapered roller bearings for the ART program. In addition, he has managed programs for bi-directional tapered roller bearings, steel and hybrid ball bearings simulating gas turbine engine main shaft applications. He received his BS in Mechanical Engineering from Pennsylvania State University

Tom Fichter is a Senior Product Development Technician employed by The Timken Company, North Canton, Ohio. He joined Timken in 1999 and provides testing support to the product and application testing group while pursuing a BS in Mechanical Engineering Technology.

ACKNOWLEDGEMENTS

The authors acknowledge the contributions of Dennis Shaughnessy of Pratt & Whitney Advanced Engine Systems for his leadership in project management and engineering support. The authors also thank Mary J. Long Davis and Isaac Lopez of the NASA Glenn Vehicle Systems Project Office for their dedicated support in program management of this research effort.